Excited-State Intramolecular Proton Transfer in 2-(2′-Acetamidophenyl)benzimidazole

Swadeshmukul Santra, G. Krishnamoorthy, and Sneh K. Dogra*

Department of Chemistry, Indian Institute of Technology Kanpur, Kanpur-208 016, India

Received: July 29, 1999; In Final Form: October 15, 1999

An excited-state intramolecular proton-transfer process has been studied in 2-(2′-acetamidophenyl)benzimidazole in different solvents using steady-state and time-resolved fluorescence spectroscopy. Semiempirical quantum mechanical calculations have also been carried out. Dual fluorescence (normal and tautomer fluorescence) is observed in all the solvents. On the basis of the fluorescence excitation spectra recorded at different wavelengths and the lifetime data, it is concluded that the normal fluorescence originates from the rotamer trans-II in aprotic solvents and the rotamers trans-II and trans-IV in protic solvents. The tautomer emission originates from the tautomer trans-III in aprotic solvents and tautomers trans-III and trans-III′ in protic solvents. The presence of an adjacent acetyl group increases the acidity of the N−H (amide proton) bond present in the phenyl ring. This leads to the faster rate of proton transfer in the S_1 state. As a result of this, the quantum yield of the tautomer band increases noticeably. With the increase of excitation wavelengths, the ratio of tautomer to normal emission increases in all the solvents. Semiempirical quantum mechanical calculations have shown that the rotamer trans-I is more stable than the rotamer trans-II in the ground state, both under isolated conditions and when dipolar solvation energy is included. Under isolated conditions the activation energy for the interconversion of rotamers is 2.9 kJ mol^{-1} in the ground state and 69.2 kJ mol^{-1} in the first excited singlet state.

1. Introduction

More than 40 years ago, Albert Weller,[1] using 2-hydroxybenzoyl compounds [Ph(OH)COR] such as methyl salicylate, laid the foundation for the subsequently called "excited-state intramolecular proton-transfer" (ESIPT) process. Since then the ESIPT phenomenon has become a field of active research.[2−10] The mechanism of the ESIPT process is currently being exploited to understand the photophysics of some compounds that exhibit such interesting properties as ultraviolet stabilization,[11,12] stimulated radiation production,[13,14] information storage,[15] fluorescent solar concentrator,[16] and environmental probes in biomolecules.[17] In organic bifunctional molecules that contain both hydrogen atom donors (e.g. −OH, $-NH_2$, etc.) and acceptors (=N−, >C=O, etc.) groups in close proximity, an intramolecular hydrogen bond (IHB) is generally formed in the electronic ground state. The intramolecular redistribution of the electronic charge due to a photonic excitation induces the ESIPT process. The most striking feature of the dynamics of these systems is the ultrafast nature of the ESIPT reaction ($k_{ESIPT} > 10^{12}$ s^{-1}) and the large Stokes shifted fluorescence (6000−10000 cm^{-1}) of the tautomer. Energetically the transfer of a normal molecule to its tautomer form is feasible in the S_1 state. The same is also true kinetically as it is well established that the rate of ESIPT reaction is very fast and is complete in less than 8 ps at room temperature.[18−20] The absolute rate of excited-state proton transfer for 2-(2′-hydroxyphenyl)benzothiazole has been determined as 170 ± 20 fs,[21] indicating that the occurrence of the proton-transfer reaction is of the order of the O−H vibrational time scale. The extreme speed is presumably due to the fact that the process involves very slight (∼1 Å) movement of a light hydrogen atom.

For the past decade our laboratory has been actively involved in investigating the excited-state reactions of organic bifunctional molecules showing ESIPT[22−26] and twisted intramolecular charge-transfer (TICT)[27,28] reactions. These molecules are mainly different derivatives of benzimidazole (BI), benzoxazole (BO), and benzothiazole (BT) moieties. Recently we have studied the photophysics of 2-(2′-aminophenyl)benzimidazole (2-APBI, Scheme 1)[23] as an extension of our earlier work.[22] We have found that 2-APBI gives dual fluorescence in nonpolar solvents. The fluorescence quantum yield and lifetime of the largely Stokes shifted band (named as the tautomer band) are very small (e.g., $\phi_{fl}^{T} = 0.005$ and $\tau = 0.85$ ns as compared to that of the normal emission $\phi_{fl}^{N} = 0.013$, $\tau_N = 1.4$ ns (70.8) and 3.48 ns (29.2), biexponential) and decrease very sharply with the increase in the polarity and hydrogen-bonding capacity of the solvents, nearly absent in water. These experimental results have been explained[23] on the basis of the following reasons: (i) the rate of ESIPT is very small when compared to its hydroxy analogue, (ii) during the lifetime of the excited state the ESIPT process is followed by twisting (Scheme 1) via path the I → III → V. This is based on our semiempirical quantum mechanical calculations, and this process is exothermic by 6.46 kJ mol^{-1} (AM1 calculation). The main reason for the slow proton transfer in 2-APBI could be due to the larger pK_a value of the $-NH_2$ group in comparison to that of the −OH group, in both the S_0 and S_1 states (>16, ∼12 for the $-NH_2$ group and ∼10, ∼0−2 for the −OH group, respectively). In the present work we have replaced one of the amino hydrogen atoms by an acetyl group (Scheme 2), keeping the following ideas in mind: (i) the electron-withdrawing acetyl group will increase the acidity of the remaining hydrogen atom on the $-NH_2$ group leading to a stronger intramolecular hydrogen bonding, (ii) the pK_a value of the neutral−monoanion (N−MA) equilibrium will be lowered further in the excited state when compared to that in 2-APBI, and (iii) the increase in the acidity of the proton donor group will lead to the faster rate of ESIPT and also increase the ϕ_{fl}^{T}.

10.1021/jp992678a CCC: $19.00
Published on Web 12/31/1999

SCHEME 1

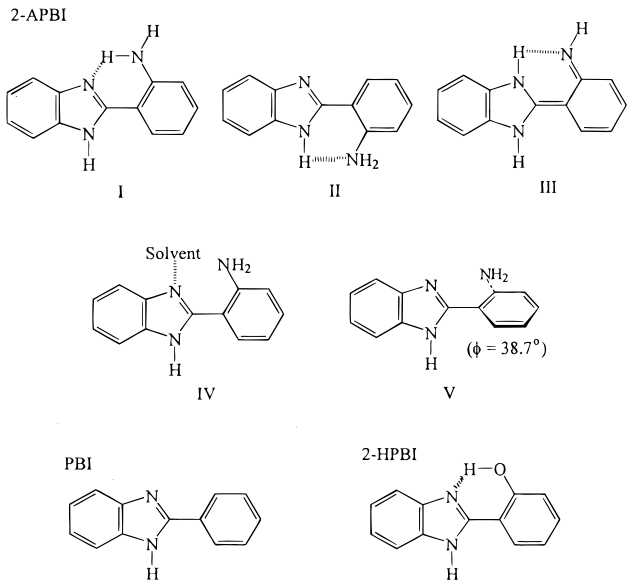

SCHEME 2

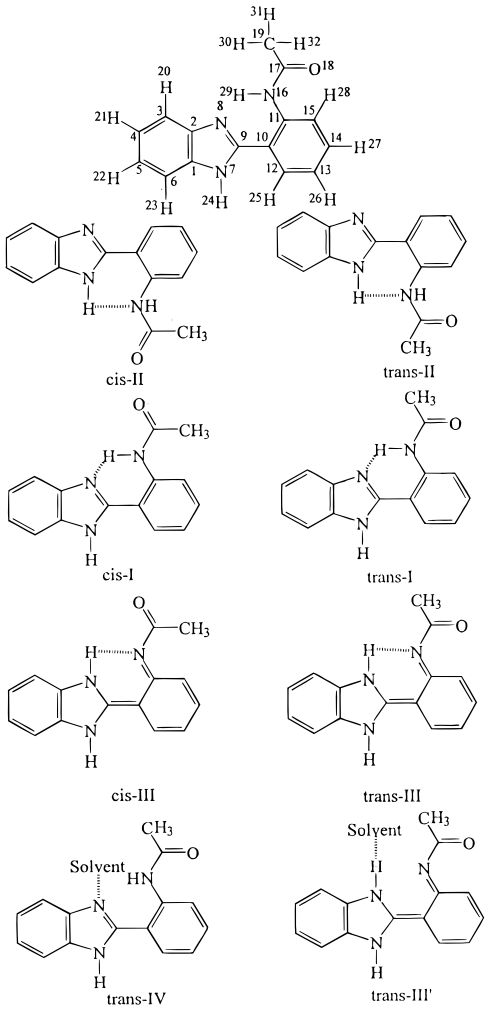

2. Materials and Methods

2-AMPBI (mp 159°) was synthesized from 2-APBI (Aldrich Chemical Co., U.K.) and acetyl chloride.[29] The product was recrystallized twice from ethanol and characterized by NMR, IR, and FAB mass spectroscopy. The purity was also checked by the production of similar fluorescence band maxima on excitation with different wavelengths of radiation. All the solvents used were either of spectroscopic grade and used as received or further purified by the methods described previously.[30] Triply distilled water was used for the preparation of aqueous solutions.

TABLE 1: Absorption Band Maxima (λ_{max}^{ab}, nm) and the Molecular Extinction Coefficient (log ϵ_{max}, L mol^{-1} cm) of 2-AMPBI in Different Solvents at 298 K

solvent	λ_{max}^{ab} (log ϵ_{max})			
cyclohexane (satd.)	289 (sh)	301	*324*	337
dioxane	289 (sh)	301 (4.26)	*322* (4.29)	335 (4.15)
ether	289 (sh)	301 (4.32)	*322* (4.35)	336 (4.24)
ethylacetate	289 (sh)	301 (4.30)	*320* (4.33)	335 (4.20)
acetonitrile	290 (sh)	301 (4.27)	*319* (4.30)	332 (4.16)
tetrahydrofuran	289 (sh)	302 (4.30)	*322* (4.34)	337 (4.21)
n-butyl alcohol	289 (sh)	302 (4.32)	*317.5* (4.37)	332 (4.25)
2-propanol	290 (sh)	302.5 (4.33)	*317.5* (4.38)	332 (4.25)
ethanol	290 (sh)	302 (4.33)	*317* (4.36)	332 (4.22)
methanol	290 (sh)	302 (4.30)	*317* (4.34)	332 (4.21)
ethylene glycol	289 (sh)	304 (4.30)	*318.5* (4.31)	333 (4.14)
glycerol	290 (sh)	302 (4.20)	317 (sh)	332.5 (sh)
water [2% methanol, (V/V)] (pH 7.0)				*293* (4.21)

Absorption spectra were recorded on a Shimadzu spectrophotometer model UV190, equipped with chart recorder model U135. Corrected fluorescence emission and excitation spectra were recorded on Fluorolog-3 model FL3-11C fluorescence spectrometer supplied by SPEX Industries Inc., U.S.A. Fluorescence quantum yields were determined with solutions having absorbance less than 0.1 and using quinine sulfate in 1 N H_2SO_4 as reference[31] ($\phi = 0.55$). Excited-state lifetimes were measured on a time-correlated single photon counting nanosecond spectrofluorimeter supplied by Applied Photophysics. Details are available in our recent paper.[32]

The PC MODEL-2 program[33] was used to find out the starting geometry of the geometrical isomers (cis and trans) of the rotamers I and II and the tautomer III (Scheme 2). This program enabled us to draw the structure, optimize roughly the geometry using MM2 force field, and generate the corresponding coordinates. The ground-state (S_0) geometries of all the species were then fully optimized by the AM1 method[34] (QCMP 137, MOPAC 6/PC). The energy of the first excited singlet state (S_1) of the respective species was calculated using the AM1 method and starting from the ground-state geometries, also known as single-point calculations. This method gives rise to the Franck−Condon state energy. Potential energy curves (PEC) were constructed in both the S_0 and S_1 states by changing the dihedral angle (ϕ) by 10° starting from both the fully optimized cis and trans isomers (see below). Transition energies for both excitation and emission were calculated in the isolated condition considering Franck−Condon states. The dipolar solvation energy[35,36] was calculated using the following equation

$$E_{solv} = -[\mu_g^2/4\pi\epsilon_0 a^3]\, f(\epsilon)$$

where $f(\epsilon) = [(\epsilon - 1)/(2\epsilon + 1)]$, μ_g is the ground-state dipole moment, a is the Onsagar cavity radius, and ϵ is the dielectric constant. The value a was calculated by taking 40% of the longer axis of the nonspherical molecules as suggested by Lippert[37] and comes out to be 4.0 Å.

3. Results

3.1. Absorption Spectra. Absorption spectra of 2-AMPBI were recorded in different solvents, and the relevant data are compiled in Table 1. Absorption spectra recorded in selected

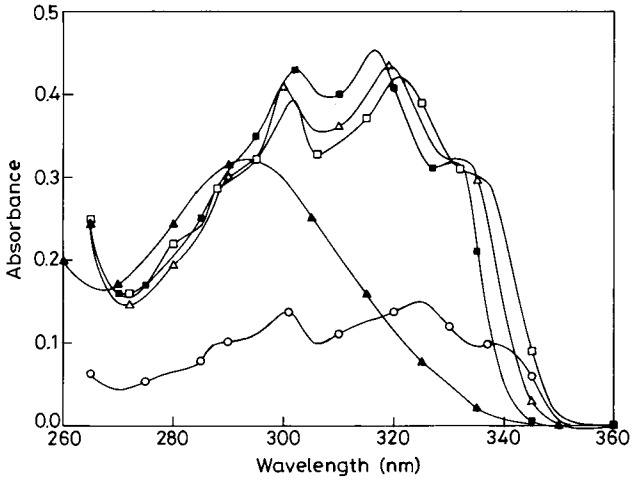

Figure 1. Absorption spectrum of 2-AMPBI in different solvents: ○, cyclohexane; □, dioxane; △, acetonitrile; ■, methanol; ▲, water. [2-AMPBI] = 2×10^{-5} M.

TABLE 2: Fluorescence Band Maxima (λ_{max}^{fl}, nm) and the Fluorescence Quantum Yield (ϕ_{fl}) of 2-AMPBI in Different Solvents, $\lambda_{exc.} = 320$ nm, [2-AMPBI] = 2×10^{-5} M

solvent	λ_{max}^{fl} (N)	ϕ_{fl} (N)	λ_{max}^{fl} (T)	ϕ_{fl} (T)	$(\phi_T/\phi_N)^a$
cyclohexane (satd.)	364	0.0015	513	0.063	42.0 (0.42)
dioxane	363	0.0008	521	0.073	91.2 (0.09)
ether	364	0.0005	515	0.097	194.0 (0.18)
ethyl acetate	373	0.002	514	0.093	46.5 (0.11)
acetonitrile	362	0.0011	512	0.097	88.2 (0.13)
tetrahydrofuran	374	0.0008	516	0.113	141.3 (0.10)
n-butyl alcohol	360	0.001	496	0.231	231.0 (0.11)
2-propanol	360	0.0005	496	0.226	452.0 (0.08)
ethanol	365	0.001	496	0.213	213.0 (0.04)
methanol	366	0.001	497	0.210	210.0
ethylene glycol	366	0.005	500	0.188	37.6
glycerol	371	0.018	495	0.199	11.1
water* [2% methanol, (V/V)]	367	0.038	473	0.059	1.6

[a] $\lambda_{exc} = 293$ nm; parentheses give (ϕ_T/ϕ_N) for 2-APBI. N = Normal band. T = Tautomer band.

solvents are shown in Figure 1. From Table 1 and Figure 1, it is clear that except in water as a solvent, the absorption maximum is red shifted with respect to 2-phenylbenzimidazole (2-PBI, Scheme 1)[38] and blue shifted with respect to the long-wavelength (LW) band of 2-APBI.[22] The absorption spectrum of 2-AMPBI is structured in nonpolar solvents and becomes diffuse with the increase in the polarity and hydrogen-bonding capacity of the solvent. With respect to the nonpolar solvents, the absorption band maxima are blue shifted by 5−6 nm in alcoholic and polar/aprotic solvents, and in water it is blue shifted by ∼44 nm with a long tail toward red.

3.2. Fluorescence Emission Spectra. Dual fluorescence was observed in all the solvents, and fluorescence bands are not structured. Fluorescence band maxima and the quantum yields are compiled in Table 2, whereas emission spectra recorded in selected solvents are shown in Figure 2. The most striking feature observed is that ϕ_{fl}^T is always larger than ϕ_{fl}^N and the ratio ϕ_{fl}^T/ϕ_{fl}^N is maximum in 2-propanol and minimum in water. These results are opposite to those observed in the case of 2-APBI in the sense that the ratio ϕ_{fl}^T/ϕ_{fl}^N in 2-APBI was always less than that in 2-AMPBI. This ratio in 2-AMPBI decreases with an increase in polarity and hydrogen-bonding nature of the solvents. Fluorescence band maxima in 2-AMPBI are blue shifted with respect to 2-APBI in any particular solvent. With the increase in the polarity and hydrogen-bonding capacity of the solvents, the band maximum of the tautomer emission gets

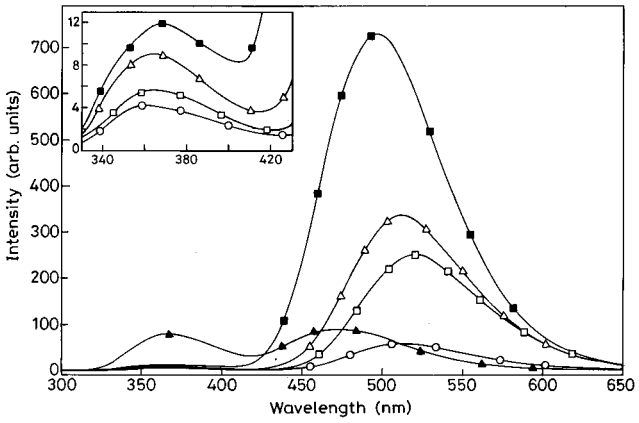

Figure 2. Fluorescence spectrum of 2-AMPBI in different solvents: ○, cyclohexane; □, dioxane; △, acetonitrile; ■, methanol; ▲, water. [2-AMPBI] = 2×10^{-5} M. Inset box shows the normal emission on the expanded scale.

TABLE 3: Fluorescence Band Maxima (λ_{max}^{fl}, nm) and Quantum Yield (ϕ_{fl}) of the Fluorescence Bands When Excited at Different Wavelengths and in Different Solvents [2-AMPBI] = 2×10^{-5} M

solvent	λ_{max}^{fl} (nm)	λ_{exc} (nm) normal	λ_{exc} (nm) tautomer	ϕ_{fl} normal	ϕ_{fl} tautomer	(ϕ_T/ϕ_N)
cyclohexane (satd.)	300	355	511	0.0026	0.077	29.6
	320	364	513	0.0015	0.063	42
	340	368	517	0.001	0.070	70
dioxane	300	363	521	0.0015	0.080	53
	320	363	521	0.0008	0.073	91.2
	340	365	521	0.0007	0.078	111.4
acetonitrile	300	363	513	0.0030	0.105	35
	320	362	512	0.0011	0.097	87.8
	340	365	512	0.0006	0.098	163
methanol	300	365	497	0.004	0.262	65.5
	320	366	497	0.001	0.265	265
	340	360	497	0.0007	0.259	370
water (pH = 7.0)	290	367	471	0.044	0.070	1.6
	310	367	480	0.029	0.068	2.4
	330	∼370	484	0.008	0.071	8.9

blue shifted whereas the band maximum of the normal band remains almost unchanged. The fluorescence spectra of 2-AMPBI were also recorded by exciting at different wavelengths in five different solvents. The data are compiled in Table 3. It is clear from the data of Table 3 that the band maxima of both the emissions were not affected much except in water, indicating that fluorescence in the rest of the solvents is occurring from the most relaxed excited singlet states in both cases. The LW fluorescence band maximum gets red shifted with the increase in the excitation wavelength. This suggests the presence of different solvated species in aqueous medium. ϕ_{fl} of the SW band decreases with the increase of excitation wavelength in each solvent, and that of the tautomer band is nearly constant. The ratio ϕ_{fl}^T/ϕ_{fl}^N is maximum in methanol when excited at the red edge of the absorption spectra and minimum in water when excited at the blue edge of the absorption spectra among the five solvents.

3.3. Fluorescence Excitation Spectra. Fluorescence excitation spectra of 2-AMPBI have been recorded at a number of wavelengths (360, 400, 420, 460, 500, 520, 540, and 580 nm) in five different solvents. Figure 3 shows the fluorescence excitation spectra recorded in cyclohexane and water using emission wavelengths as 360 and 500 nm. The fluorescence excitation spectrum recorded at the tautomer emission in cyclohexane is structured, indicating that the rotamer responsible for this emission is quite rigid, whereas the fluorescence spectra recorded in other solvents at other emission wavelengths are

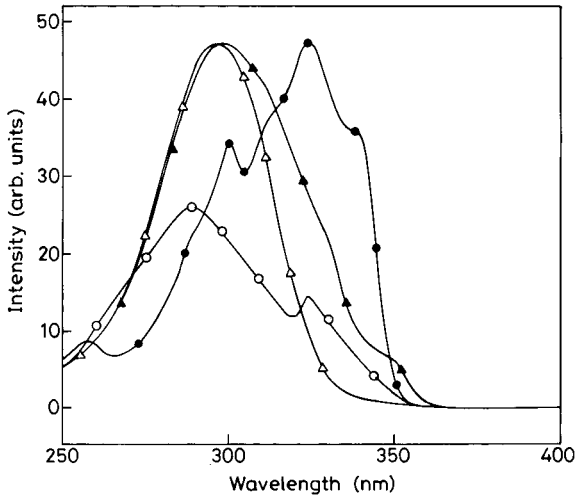

Figure 3. Fluorescence excitation spectrum of 2-AMPBI in cyclohexane ○, $\lambda_{em} = 360$ nm; ●, $\lambda_{em} = 500$ nm and in water △, $\lambda_{em} = 360$ nm; ▲, $\lambda_{em} = 500$ nm.

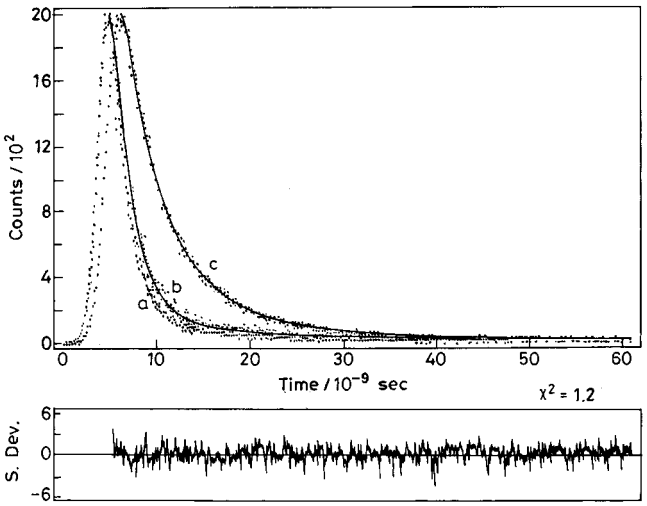

Figure 4. Fluorescence decay curves of 2-AMPBI in water (a) lamp profile, monitoring at (b) 365 nm (normal band) and (c) 480 nm (tautomer band). $\lambda_{exc} = 311$ nm, [2-AMPBI] $= 4 \times 10^{-5}$ M.

broad. From Figure 3 it is quite clear that two distinct species of 2-AMPBI are present in the ground state and the absorption spectrum of 2-AMPBI is a mixture of the absorption spectra of these two species.

3.4. Excited-State Lifetimes. Excited-state lifetimes were measured in different solvents and at different emission wavelengths of the large Stokes shifted tautomer fluorescence band. Figure 4 represents the fluorescence decay of both the bands in water, and the relevant data are compiled in Table 4. We could record the same for the normal emission only in water containing 2% methanol (v/v) because of its weak fluorescence intensity in other solvents. The normal emission follows a double exponential, as observed in case of 2-HPBI[39] and 2-APBI.[23] The tautomer emission follows a single exponential in non-hydrogen-bonding solvents and double-exponential decay in methanol and water.

3.5. Quantum Mechanical Calculations. 2-AMPBI can have two different rotamers (I and II) and one tautomer (III) as shown in Scheme 2. Each rotamer and tautomer can also be represented by two geometrical isomers. When >NH and >C═O groups are on the same side, it is represented as a cis isomer, and as a trans isomer when these two groups are on the opposite side. Therefore there are six plausible structures of 2-AMPBI. All

TABLE 4: Lifetimes Values (τ ns) of the Tautomer Band of 2-AMPBI in Different Solvents and Measured at Different Emission at $\lambda_{exc} = 332$ nm (Except in Water Where $\lambda_{exc} = 311$ nm)

		fit 1		fit 2				
solvent	λ_{em}	τ	χ^2	τ_1	a_1	τ_2	a_2	χ^2
cyclohexane	500	1.96	1.2					
dioxane	480	2.10	1.20					
	520	1.90	1.20					
	560	2.10	1.14					
aceonitrile	480	2.46	1.05					
	520	2.44	1.19					
	560	2.30	1.05					
methanol	500	3.30	1.40	1.54	33.1	4.0	66.1	1.24
	530	3.52	1.44	1.48	18.5	3.9	81.5	1.30
	560	3.40	1.56	1.52	16.0	4.1	84.0	1.20
water	365[a]	0.56	1.61	0.43	86.7	6.66	13.3	1.20
	480	4.39	1.47	0.71	42.2	4.70	57.8	1.21
	520			0.80	48.2	4.60	51.8	1.23

[a] This is a normal emission band. Fit 1 and Fit 2 are single and double exponential.

these structures have been fully optimized in the ground state by the AM1 method,[34] and the relevant data are compiled in Table 5. Theoretical parameters of the tautomer III in the S_1 state were also calculated using the ground-state configurations, known as single-point calculations (QCMP137, MOPAC 6/PC). The data are also compiled in Table 5. Potential energy curves for the interconversion of the rotamer I to rotamer II were also constructed (Figure 5) in both the S_0 and S_1 states varying ϕ by 10° in the range of 0°−180° starting from both cis and trans geometries. Plots a and a′ represent the plots of interconversion of the trans isomer, whereas plots b and b′ show the plots of interconversion of the cis isomer. The energy level diagrams depicting the absorption and fluorescence processes for different species have been drawn in Figure 6.

4. Discussion

Out of six structures (Table 5), both the cis and trans tautomer structures are highly unstable with respect to trans-I by 104.2 and 94.6 kJ mol^{-1}, respectively, under isolated conditions and by 80.4 and 42.6 kJ mol^{-1}, respectively, when dipolar solvation energy is taken into account. Under such conditions the presence of the tautomers can be neglected in the S_0 state. Further under isolated conditions and in the S_0 state, the trans-I and trans-II isomers are more stable than the cis-I and cis-II isomers by 7.83 and 9.9 kJ mol^{-1}, respectively. Similarly in the S_1 state, the stability of the trans-I and the trans-II isomers over the cis-I and the cis-II isomers is 13.6 and 7.5 kJ mol^{-1}, respectively. The lesser stability of the cis isomers in comparison to the trans ones is because of the close proximity of the lone pairs of electrons on the N_{16} atom (Scheme 2) and the adjacent carbonyl oxygen atom in the cis forms, whereas in the trans forms the lone pairs of electrons on both the atoms are projected in opposite directions. This will lead to less repulsive force in the trans rotamers than in the cis rotamers. Thus, on the basis of the Maxwell−Boltzmann distribution, the populations of the rotamers trans-II, cis-I, and cis-II with respect to the rotamer trans-I under isolated conditions would be 0.46, 0.043, and 0.009, respectively. Relative stability of the cis isomers over the trans isomers in the S_0 state will increase with the increase in the polarity and hydrogen-bond-forming capacity of the solvents if the solvation energies due to the dipolar interaction (eq 1) are taken into account. This is because the μ_g's of the rotamers cis-I and cis-II are larger than that of the rotamer trans-I. On the basis of the above calculations, it appears that

TABLE 5: Calculated Parameters of Different Rotamers and Tautomers of the cis- and trans- 2AMPBI in the S_0 and S_1 States Using the AM1 Method (MOPAC 6.0)

	rotamer					
	trans II		trans I		tautomer-III (trans)	
parameters	S_0	S_1	S_0	S_1	S_0	S_1
E_{isol} (eV)	−3039.100	−3035.178	−3039.120	−3035.429	−3038.139	−3035.557
E_{solv} (eV)	−3039.157	−3035.288	−3039.193	−3035.550	−3038.752	−3035.802
$r(C_9-C_{10}$, nm)	0.147	0.147	0.147	0.147	0.142	0.142
r(H-bond, nm)	$N_{16}-H_{24}$	$N_{16}-H_{22}$	N_8-H_{29}	N_8-H_{29}	$N_{16}-H_{29}$	$N_{16}-H_{29}$
	0.310	0.262	0.235	0.212	0.210	0.210
ϕ ($C_{11}-C_{10}-C_9-N_8$)	−60	−20	52	10	3.2	3.2
μ (D)	2.44	3.34	2.74	3.56	8.0	5.0
charge densities	5.2407	5.2770	5.2337	5.2663	5.2544	5.2155
N_7	5.1231	5.1227	5.1579	5.1902	5.2108	5.1726
N_8	5.3368	5.3102	5.3275	5.2577	5.4380	5.3045
N_{16}	6.3496	6.3430	6.3569	6.3414	6.3858	6.3610
O_{18}						

	rotamer					
	cis-II		cis-I		tautomer-III (cis)	
parameters	S_0	S_1	S_0	S_1	S_0	S_1
E_{iso} (eV)	−3038.997	−3035.100	−3039.039	−3035.288	−3038.040	−3035.389
E_{sol} (eV)	−3039.088	−3035.122	−3039.292	−3035.495	−3038.360	−3035.555
ϕ	−40	0.0	50	10	3.0	3.0
μ (D)	3.07	1.53	5.11	4.65	5.76	4.15

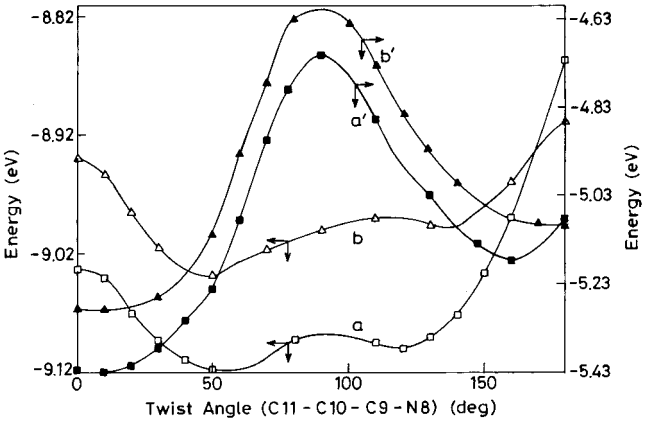

Figure 5. Potential energy curves for 2-AMPBI as an isolated molecule for the cis and trans isomers in the S_0 and S_1 states. □, trans, S_0; ■, trans S_1; △, cis, S_0; ▲, cis, S_1.

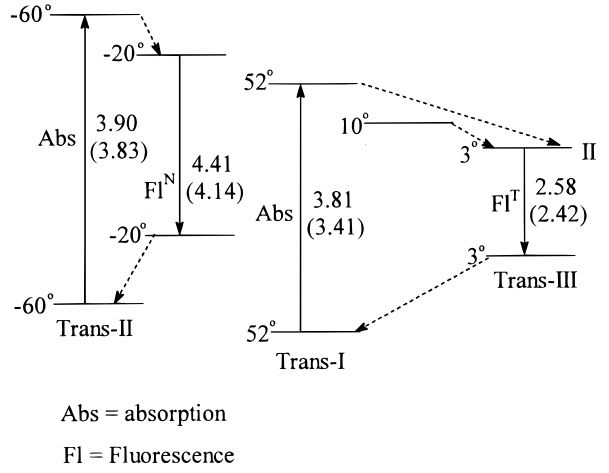

Figure 6. Energy of the rotamers trans-I, trans-II and tautomer trans-III of 2-AMPBI under isolated conditions. The values in parentheses are experimental values.

in the ground state all the four possible rotamers (cis-I, cis-II, trans-I, and trans-II) can exist and the proportion of the cis rotamers will increase with the increase in the polarity of the solvents.

It is now well established that the normal fluorescence is only observed from the rotamers of type II and/or from the rotamers of type IV[2−10] (Scheme 1), whereas the tautomer emission is only observed from the rotamers of type-I, after undergoing ESIPT. On the basis of the results of Table 5, the normal fluorescence spectrum of rotamer trans-II of 2-AMPBI would have been slightly red shifted ($\mu_g = 2.44$ D, $\mu_e = 3.34$ D) with the increase in the polarity of the solvents, and the normal fluorescence spectrum of rotamer cis-II would have been largely blue shifted ($\mu_g = 3.07$ D, $\mu_e = 1.53$ D) under the above conditions. The results of Table 2 clearly show that the normal emission is either invariant or a slight red shift is observed under the above environments. Similarly, the results of Table 5 also suggest that the fluorescence band maximum of the trans-tautomer-III will be largely blue shifted ($\mu_g = 8.0$ D, $\mu_e = 5.0$ D) in comparison to that of cis-tautomer-III ($\mu_g = 5.76$ D, $\mu_e = 4.15$ D). The results of Table 2 clearly indicate that the fluorescence band maximum of the tautomer band is blue shifted from 513 nm in cyclohexane to 473 nm in water. Although the dipole moment of the cis-tautomer-III also decreases on excitation to S_1, the decrease is not as large as that observed in the trans-tautomer-III. Thus it may be concluded that in the ground state, 2-AMPBI exists as the rotamers trans-I and trans-II. This is substantiated by the fact that the rotamer trans-I is more stable than the trans-II by only 1.9 kJ mol^{-1} and the barrier height for the interconversion of the trans-I to the trans-II in the ground state is only 2.9 kJ mol^{-1} under isolated conditions. Thus at room temperature the interconversion between the two rotamers is possible and the relative populations of the trans-I and trans-II, under isolated conditions and using Boltzmann distribution, would be in the ratio of 1:0.46. Further it may also be pointed out that the stability of the rotamer trans-I and the barrier height for the conversion of the trans-I to the trans-II both in the S_0 and S_1 states will increase in polar solvents when solvation energies are included, because the dipole moments (μ_g, μ_e) of the trans-I (2.74 D, 3.56 D) are greater than those of the trans-

II (2.43 D, 3.34 D). It may also be pointed out that unlike 2-APBI[23] and 2-HPBI,[39] the rotamer trans-I is more stable than the trans-II in 2-AMPBI under isolated as well as solvated conditions. This could be because of the presence of stronger IHB in the rotamer trans-I than that in the rotamer trans-II. This is substantiated by (i) the shorter bond distance between amino proton and $=N_8-$ atom (0.235 nm) than between $>N-H$ and amino nitrogen atom (0.310 nm), (ii) smaller dihedral angle ϕ in trans-I (52°) than that in trans-II (−60°), and (iii) the presence of structure in the fluorescence excitation spectrum recorded at the tautomer emission, orginating from the rotamer I after ESIPT reaction.

Having established that 2-AMPBI will be present in the trans form only, we can explain the rest of the photophysical properties taking this isomer into consideration. Large values of the molecular extinction coefficients and the moderate ϕ_{fl} establish that the lowest energy electronic transition in 2-AMPBI is of $\pi \rightarrow p^*$ in nature in all the solvents. The blue shift observed in the LW absorption band maximum of 2-AMPBI in comparison to 2-APBI in any particular solvent is due to the fact that the lone pair of electrons on the amino nitrogen atom will be involved in the resonance effect with the carbonyl π-cloud, as well as with the π-cloud of the aromatic moiety. On the other hand, the red shift in the LW absorption band maximum of 2-AMPBI in comparison to 2-PBI[38] confirms the presence of IHB in 2-AMPBI. This rigidity in the structures of the rotamers is substantiated by the presence of structure in the absorption and fluorescence excitation spectrum recorded at the 500 nm band of 2-AMPBI in nonpolar and less polar solvents. Absence of the vibrational structure in the LW absorption band of 2-AMPBI in water (Table 1) suggests that the intermolecular hydrogen bonding of 2-AMPBI with water is stronger than the intramolecular hydrogen bonding. This is substantiated by the fact that the fluorescence quantum yield of the normal band increases by a factor of ∼4 in going from methanol to water, suggesting an increase in the population of the rotamer trans-IV at the expense of rotamer trans-I. The disagreement between the fluorescence excitation spectra when recorded at different emission wavelengths with the absorption spectrum of 2-AMPBI is due to the presence of two species in the ground state. In other words, the absorption spectrum of 2-AMPBI is a mixture of the absorption spectra of the two rotamers. The individual band maximum obtained from the fluorescence excitation spectra agrees nicely with those obtained from theoretical calculations (Figure 6); i.e., the 324 nm band maximum can be assigned to the rotamer trans-I and the 290 nm band maximum to the rotamer trans-II.

Unlike with 2-APBI, the results of Table 2 show that ϕ_{fl}^T is always larger than ϕ_{fl}^N in all the solvents. This is primarily due to the increase in the acidity of the amino hydrogen atom. The presence of the electron-withdrawing carbonyl group will increase the acidity of the amino hydrogen atom in both the S_0 and S_1 states; e.g., the pK_a value for the deprotonation of the amide group in the S_0 state is 11.8.[40] Although the fluorimetric titrations have indicated that the deprotonation equilibrium is not established in the S_1 state during the lifetime of the excited species, the Forster cycle method has shown that pK_a* for the deprotonation reaction is 7.0. On the other hand, for the amino group, the pK_a and pK_a* values are >16 and 12.8.[22] Semiempirical quantum mechanical calculations also substantiate this; i.e., (i) in the trans-I rotamer, there is a decrease of charge density on N_{16} by 0.0698 unit and on H_{29} (hydrogen-atom-bonded to N_8) by 0.01 unit, and an increase in the charge density on N_8 by 0.0323 unit, and (ii) the intramolecular hydrogen-bonding distance (N_8-H_{29}, 0.21) in 2-AMPBI is slightly less than that in 2-APBI (0.22 nm). The other reason for the increase in ϕ_{fl}^T could be due to the decrease in the rate of the nonradiative process as the tautomer is more planar (ϕ decreases from 52° to 3.2°) than the rotamer trans-I in the S_1 state. This is in agreement with the well-known fact[41] that the reduction in the flexibility of the molecule in the S_1 state decreases the nonradiative decay constant. The decrease in the ϕ_{fl}^T in water is due to the formation of the rotamer trans-IV (Scheme 2) at the expense of rotamer trans-I (see below). The decrease in the fluorescence quantum yield of the normal emission with increase in λ_{exc} suggests a decrease in the gap between the normal S_1 state and the low-lying triplet state of the rotamer trans-II, and thereby an increase in the intersystem crossing rate. On the other hand, the invariance of ϕ_{fl}^T with λ_{exc} suggests that the intersystem crossing rates to the low-lying triplet states are not affected by λ_{exc}.

AM1 calculations have shown that the tautomer trans-III is more stable than the rotamer trans-I by 12.42 kJ mol^{-1} under isolated conditions and 24.32 kJ mol^{-1} when dipolar solvation energy is included in the S_1 state. Thus ESIPT is the major pathway for the deactivation of the rotamer trans-I to the tautomer trans-III. Two distinct fluorescence bands and distinct fluorescence excitation spectra in all the solvents (including ultradry hydrocarbons) clearly establish the presence of at least two distinctly different species in the S_0 state. Two possible trans rotamers (II and IV) can lead to the normal fluorescence, as shown by the earlier studies.[39,42−44] The rotamer trans-IV will be present only in highly polar and protic solvents, whereas the rotamer trans-II can exist only in dry nonpolar solvents or in polar/protic solvents where the intermolecular hydrogen bonding is weaker than the intramolecular hydrogen bonding. Since the normal fluorescence is also observed in pure and dry nonpolar solvents, we conclude that in nonpolar solvents the normal fluorescence originates only from the rotamer trans-II and the tautomer fluorescence from the rotamer trans-I. On the other hand, in protic solvents such as water, normal emission is observed from the rotamers trans-II and trans-IV. The double-exponential decay observed in the normal emission in water substantiates this. Further, in the ground state, the interconversion of the rotamer trans-I to trans-II is possible because of the smaller activation barrier (2.9 kJ mol^{-1}), whereas this interconversion cannot occur in the S_1 state as the activation barrier for their transformation increases to 69.2 kJ mol^{-1}. This is confirmed by the different lifetimes observed for the normal and tautomer emission, suggesting that the equilibrium is not established between the two rotamers in the S_1 state. Single-exponential decay observed in the tautomer emission of 2-AMPBI in nonprotic solvents indicates the presence of only one form of the tautomer trans-III, whereas the double-exponential decay observed in polar/protic solvents in the tautomer trans-III emission suggests the presence of two species (Scheme 2). Although the detailed study is needed in the binary solvents, the preliminary study suggests the presence of two types of tautomers, trans-III, a closed structure, and trans-III′, a solvated structure. The shorter lifetime can be assigned to the solvated tautomer trans-III′ as its proportion (amplitude) increases in going from methanol to water. A similar behavior is also observed by Robert et al.[45] in 2-HPBI.

The fluorescence quantum yield of the fluorophore depends on the population of the fluorophore in the ground state and the rates of nonradiative decay processes. The increases in the

lifetime and the fluorescence quantum yield of the tautomer band in going from cyclohexane to acetonitrile (Table 4) suggest the decrease in the nonradiative decay rate, whereas in methanol and water it is opposite. Further, the amplitude of the long-lived species in methanol is larger than that of the short-lived species, and in water the two amplitudes are nearly equal. On the basis of the results of Table 5 and from the above explanation, it can be concluded that the large increase in ϕ_{fl}^{T} up to 2-propanol is due to the decrease in k_{nr} and the relative increase in the population of the rotamer trans-I over the rotamer trans-II, whereas in methanol and water, the decrease in ϕ_{fl}^{T} is due to the increase in the population of the rotamer trans-IV at the expense of the rotamer trans-I, as well as to the increase in the k_{nr} in water only. However, the increase in the ϕ_{fl}^{N} value in polar/protic solvents is due to the increase in the population of the rotamer IV at the expense of the rotamer trans-I (specially) and the rotamer trans-II. In other words, in polar/protic solvents (especially water), besides the rotamer trans-II, normal emission is also observed from the solvated rotamer trans-IV. This is reflected by the biexponential decay observed in the normal emission in water. This will lead to the decrease in ϕ_{fl}^{T} (as explained earlier) and increase in ϕ_{fl}^{N}. Near similarity of the fluorescence band maxima originating from either II or IV can be seen from the near similar fluorescence excitation band maxima obtained in cyclohexane (290 nm) and water (296 nm) when recorded at normal emission and also agreeing with the absorption spectra.

Last, on the basis of the above results, it may be concluded that the tautomer emission in 2-AMPBI does not involve the presence of structure V (Scheme 1) because, unlike 2-APBI, the energy of the tautomer trans-III is lower than that of the rotamer trans-I and thus the ESIPT process in the rotamer trans-I will be exothermic.

Conclusion

The above study reveals that (i) combining the results of the semiempirical quantum mechanical calculations and the experimental observations, only the trans form of 2-AMPBI is present in the S_0 state, (ii) two distinct rotamers of 2-AMPBI are present in the ground state, and the absorption spectrum is a mixture of the absorption spectra of the two rotamers; the 324 nm band maximum is assigned to the rotamer trans-I and 290 nm to the rotamer trans-II, (iii) the rotamer trans-I is more stable than the rotamer trans-II under isolated and solvated conditions because of the stronger intramolecular hydrogen bonding. This is due to the appreciable increase in the acidity of the amino proton caused by the presence of the electron-withdrawing carbonyl group, (iv) the increase in the ϕ_{fl}^{T} is due to the decrease in the pK_a and pK_a^* values of the deprotonation constant and thus increase in the rate of proton transfer, and (v) the tautomer emission is assigned to the tautomer trans-III, orginating from the rotamer trans-I in aprotic solvents, whereas in protic solvents it is due to the tautomer trans-III and solvated trans-III′. The normal emission in dry nonpolar solvents is from the rotamer trans-II and both trans-II and trans-IV in polar/protic solvents.

Acknowledgment. The authors are thankful to the Department of Science and Technology, New Delhi, for the financial support of the project no. SP/SI/H-39/96.

References and Notes

(1) Weller, A. *Z. Electrochem.* **1956**, *60*, 1144.
(2) Douhal, A.; Amat-Guerri, F.; Acuna, A. U. *J. Phys. Chem.* **1995**, *99*, 76.
(3) Douhal, A.; Lahmani, F.; Zewail, A. H. *Chem. Phys.* **1996**, *207*, 477 and references listed therein.
(4) Arnaut L. G.; Formosinho, S. J. *J. Photochem. Photobiol. A* **1993**, *75*, 1.
(5) Formosinho S. J.; Arnaut, L. G. *J. Photochem. Photobiol. A* **1993**, *75*, 21.
(6) English, D. S.; Zhang, W.; Kraus G. A.; Petrich, J. W. *J. Am. Chem. Soc.* **1997**, *119*, 2980.
(7) Thoburn, H. D.; Luttke, W.; Benedict D.; Limbach, H. *J. Am. Chem. Soc.* **1996**, *118*, 12459.
(8) Sekikawa, T.; Kobayashi T.; Inabe, T. *J. Phys. Chem. A* **1997**, *101*, 644.
(9) Douhal, A.; Amat-Guerri, F.; Acuna, A. U. *Angew Chem., Int. Ed. Engl.* **1997**, *36*, 1514.
(10) Douhal, A. *Science* **1997**, *276*, 221.
(11) Catalan J.; Del Valle, J. C. *J. Am. Chem. Soc.* **1993**, *115*, 4321.
(12) Catalan, J.; Del Valle, J. C.; Claramunt, R. M.; Sanz D.; Dotor, J. *J. Lumin.* **1996**, *68*, 165.
(13) Khan, A. U.; Kasha, M. *Proc. Natl. Acad. Sci. U.S.A.* **1983**, *80*, 1767.
(14) Acuna, A. U.; Amat-Guerri, F., Catalan, J., Costella, A., Figuerra, J. M.; Munoj, J. *Chem. Phys. Lett.* **1986**, *132*, 567.
(15) Munn, R. W. *Chem. Br.* **1989**, 517.
(16) Vollmer, F.; Rettig, W. *J. Photochem. Photobiol. A* **1996**, *95*, 143.
(17) Sytnik, A.; Kasha, M. *Proc. Natl. Acad. Sci. U.S.A.* **1994**, *91*, 8627.
(18) Barbara, P. F.; Brus, L. E.; Rentzepis, P. M. *J. Am. Chem. Soc.* **1980**, *102*, 5631; *J. Am. Chem. Soc.* **1980**, *102*, 2786.
(19) McMorrow, D.; Kasha, M. *J. Phys. Chem.* **1984**, *88*, 2235.
(20) Dick, B.; Ernsting, N. P. *J. Phys. Chem.* **1987**, *91*, 4261.
(21) Larmer, F.; Elsaesser, T.; Kaiser, W. *Chem. Phys. Lett.* **1988**, *148*, 119.
(22) Santra, S.; Dogra, S. K. *Chem. Phys.* **1998**, *226*, 285.
(23) Mishra, A. K.; Dogra, S. K. *J. Photochem.* **1985**, *31*, 333.
(24) Sinha, H. K.; Dogra, S. K. *Chem. Phys.* **1986**, *102*, 337.
(25) Krishnamurthy, M.; Dogra, S. K. *J. Photochem. Photobiol.* **1985**, *32*, 235.
(26) Santra, S.; Dogra, S. K. *J. Mol. Struct.* **1999**, *476*, 223.
(27) Dey, J. K.; Dogra, S. K. *J. Phys. Chem.* **1994**, *98*, 3638.
(28) Krishnamoorthy, G.; Dogra, S. K. *Chem. Phys.* **1999**, *243*, 45.
(29) *Vogel's Text Book of Practical Organic Chemistry Including Qualitative Organic Analysis*, 4th ed.; Revised by Furniss, B. S.; Hannaford, A. J.; Rogers, V.; Smith, P. W. G.; Tatchell, A. R. ELBS, Longman: Essex, U.K., 1978; p 682.
(30) Riddick, J. A.; Bunger, W. B. *Organic Solvents*; Wiley-Interscience: New York, 1970.
(31) Guilbault, G. G. *Practical Fluorescence*; Dekker: New York, 1971; p 13.
(32) Sarpal, R. S.; Dogra, S. K. *J. Chem. Soc., Faraday Trans. 1* **1992**, *88*, 2725.
(33) Tai, J. C.; Allinger, N. L. *J. Am. Chem. Soc.* **1980**, *110*, 2050.
(34) Dewar, M. J. S.; Zoebish, E. G.; Healy, E. F.; Stewart, J. J. P. *J. Am. Chem. Soc.* **1985**, *107*, 3902.
(35) Mataga, N.; Kubato, T. *Molecular Interactions and Electronic Spectra*; Marcel Dekker: New York, 1970.
(36) Letard, J. F.; Lapouyada, R.; Rettig, W. *Chem. Phys. Lett.* **1994**, *222*, 2091.
(37) Lippert, E. Z. *Naturforsch., A* **1955**, *10*, 541.
(38) Mishra, A. K.; Dogra, S. K. *Spectrochim. Acta* **1983**, *39A*, 609.
(39) Das, K.; Sarkar, N.; Ghosh, A. K.; Majumdar, D.; Nath, D. N.; Bhattacharyya, K. *J. Phys. Chem.* **1994**, *98*, 9126.
(40) Santra, S.; Krishnamoorthy, G.; Dogra, S. K. Unpublished results.
(41) Saha, S. K.; Dogra, S. K. *J. Photochem. Photobiol. A* **1997**, *110*, 257.
(42) Schwartz, B. J.; Peteanu, L. A.; Harris, C. B. *J. Phys. Chem.* **1992**, *96*, 3591.
(43) Peteanu, L. A.; Mathies, R. A. *J. Phys. Chem.* **1992**, *96*, 6910.
(44) Chou, P. T.; Martinez, M. L.; Clements, J. H. *J. Phys. Chem.* **1993**, *97*, 2618 and references listed therein.
(45) Robert, E. L.; Dey, J. K.; Warner, I. M. *J. Phys. Chem.* **1997**, *101*, 5296.